

THE PENNSYLVANIA STATE UNIVERSITY  
SCHREYER HONORS COLLEGE

DEPARTMENT OF CHEMICAL ENGINEERING

SELF-ASSEMBLY OF AMPHIPHILIC NANOPARTICLES AND TUBULES

SEAN AUSTIN LEWIS  
SPRING 2013

A thesis  
submitted in partial fulfillment  
of the requirements  
for a baccalaureate degree  
in Chemical Engineering  
with honors in Chemical Engineering

Reviewed and approved\* by the following:

Kyle Bishop  
Assistant Professor of Chemical Engineering  
Thesis Supervisor

Wayne Curtis  
Professor of Chemical Engineering  
Honors Adviser

\*Signatures are on file in the Schreyer Honors College

## ABSTRACT

Molecular amphiphiles organize spontaneously to form diverse molecular assemblies – micelles, vesicles, and bilayers – through the competition of attractive and repulsive forces between their hydrophilic and hydrophobic components and the surrounding environment. By analogy, nanostructures functionalized with hydrophilic and hydrophobic domains should allow for the programmable assembly of nano-scale components into various higher order structures depending on the shape of the formative units and their surface chemistry. In this thesis, I describe two such colloidal amphiphiles: 1) spherical nanoparticles functionalized with hydrophilic and hydrophobic ligands capable of dynamic redistribution and 2) cylindrical tubules with hydrophobic interiors and hydrophobic exteriors (or vice versa).

In the first set of experiments, gold nanoparticles functionalized with mixed hydrophilic and hydrophobic ligands were successfully incorporated into the membrane bilayers of surfactant vesicles. Because the ligands will redistribute in response to environmental stimuli, the hydrophobic ligands can rearrange to interact with the hydrophobic membrane core and tether the nanoparticle to the vesicle. In contrast to previous reports, the size of these nanoparticles may be larger than the bilayer thickness, and the spontaneous integration upon simple mixing eliminates any membrane denaturing requirements.

In the second set of experiments, tubules of nanometer, micrometer, and millimeter diameters with differing internal and external functionalization were examined in the presence of aqueous and organic fluids to determine their potential to assemble end-on-end into chains. Desired solvents or materials could then be transported through the channels formed by these tubules. Solvent contained within each tubule by hydrophobic or hydrophilic interactions should guide the association of the open ends of each tube through the formation of capillary “bridges”

by minimizing their interfacial surface tension when submerged in solution. While macro-scale tests demonstrate some favorable interactions by forcep-assisted manual manipulation – tubules can drag one another through water when connected by toluene exposed at their open ends – further experiments are required to test of the validity of their usage and self-assembly.

Supramolecular structures created from these amphiphiles are useful most notably for controlled particle transport. By modifying the specific ligands, desired substances can be loaded into vesicles or tubules and then directed or released via external forces (such as ultraviolet or infrared light for nanoparticles and solvent flow or local variations in surface energy in the case of tubules). Future experiments will focus on integrating magnetic materials into these systems for targeted delivery applications.

## TABLE OF CONTENTS

List of Figures.....	iv
Acknowledgements.....	v
Chapter 1: Research Overview.....	1-4
Research Motivation.....	1
Research Objectives.....	4
Chapter 2: Relevant Literature on Amphiphilic Structures and their Self-Assembly.....	5-9
Previous Nanoparticle Research.....	5-7
Amphiphilic NPs at a Liquid-Liquid Interface.....	5
Membrane Penetration by Monolayer-Protected NPs.....	6
Lipid/QD Hybrids for Cell Targeting.....	6
Hydrophobic AuNP Assembly with Vesicles.....	7
Previous Tubule Research.....	8-9
Magnetics NTs for Biointeraction and Drug Delivery.....	8
Anisotropic Particles at an Oil-Water Interface.....	8
Cylindrical Particle Assembly by Capillary Interactions.....	9
Chapter 3: Experimental Procedures.....	10-15
Nanoparticles.....	10-12
AuDDA NP Seed Solution.....	10
AuDDA NP Growth Solution.....	10
Precipitation and Concentration Determination of AuDDA NPs.....	11
Functionalization of AuMUA/ODT NPs.....	11
Vesicle Synthesis and NP Mixing.....	12
Tubules.....	13-15
Au/Fe <sub>2</sub> O <sub>3</sub> Tubules from Electrospun Fibers.....	13
SiO <sub>2</sub> /Fe <sub>3</sub> O <sub>4</sub> NTs from Alumina Templates.....	14
Glass Tubes with Hydrophobic Interiors.....	15
Chapter 4: Results and Discussion.....	16-25
Nanoparticles.....	16-20
Tubules.....	21-25
Chapter 5: Conclusion.....	26
References.....	27-28

## LIST OF FIGURES

Figure 1.1: Amphiphilic nanoparticle incorporation into surfactant vesicle schematic.

Figure 1.2: Amphiphilic tubule arrangement into chains schematic.

Figure 3.1: AuMUA/ODT NP schematic.

Figure 3.2: AuMUA/ODT NP association with surfactant vesicle schematic.

Figure 3.3: Au/Fe<sub>2</sub>O<sub>3</sub> Tubules from electrospun polycarbonate fiber schematic.

Figure 3.4: SiO<sub>2</sub>/Fe<sub>3</sub>O<sub>4</sub> nanotubes from alumina template schematic.

Figure 4.1: TEM and Cryo-TEM images of AuMUA/ODT NPs.

Figure 4.2: TEM imagery for AuMUA NPs and DLS data for AuMUA and AuMUA/ODT NPs in pH 11 water.

Figure 4.3: TEM imagery of AuMUA NPs and Cryo-TEM imagery of AuMUA NPs with surfactant vesicles.

Figure 4.4: Cryo-TEM imagery of AuMUA/ODT NPs without added salt and Zeta-potential data for AuMUA/ODT NPs mixed with surfactant vesicles with and without salt.

Figure 4.5: SEM images of Au coated PC fibers, Au tubules, Fe<sub>2</sub>O<sub>3</sub> coated PC fibers, Fe<sub>2</sub>O<sub>3</sub> tubules, Au/Fe<sub>2</sub>O<sub>3</sub> coated PC fibers, and Au/Fe<sub>2</sub>O<sub>3</sub> tubules.

Figure 4.6: EDS spectrum for Au/Fe<sub>2</sub>O<sub>3</sub> tubules.

Figure 4.7: Microscope images of SiO<sub>2</sub>/Fe<sub>3</sub>O<sub>4</sub> nanotubes dispersed in water.

Figure 4.8: SEM images of alumina template after SiO<sub>2</sub> and Fe<sub>3</sub>O<sub>4</sub> deposition with and without polishing by SiC pellets.

Figure 4.9: TEM images of SiO<sub>2</sub> only nanotubes and SiO<sub>2</sub>/Fe<sub>3</sub>O<sub>4</sub> nanotubes.

## **ACKNOWLEDGEMENTS**

I would like to thank my thesis supervisor, Dr. Kyle Bishop, and my postdoctoral mentor, Dr. Hee Young Lee, for all of their help developing my experimental skills and research knowledge, as well as for their vocational guidance and advice. I would also like to extend my gratitude to the rest of our laboratory group for their assistance and amity over the course of the past few years.

## CHAPTER 1

### Research Overview

This chapter presents the research impetus and objectives involved in the experimental analysis of the amphiphilic self-assembly of spherical particles and cylindrical tubules.

### Research Motivation

An amphiphilic structure describes any molecule or material that has covalently bonded hydrophilic (soluble in water) and hydrophobic (insoluble in water) groups. When introduced into an environment containing both hydrophilic and hydrophobic regions, these groups relocate to maximize favorable interactions with their preferred local environment. This spontaneous association forms the basis for general amphiphilic self-assembly<sup>1</sup>. Various supramolecular structures created via this phenomenon are used in a variety of applications as diagnostic imaging agents<sup>2</sup>, vessels for chemical reactions<sup>3</sup>, molecular sensors<sup>4</sup>, and drug carriers<sup>5</sup>.

Controlling the actual movement of these assemblies to a desired location remains difficult, however, due to the need for powerful external driving forces (such as magnetic fields or ultraviolet/infrared light sources) which is further complicated by the fact that most amphiphilic molecules exist at the nano-scale<sup>6</sup>. Ameliorating this issue to develop improved control over particle transport was thus the primary goal of this research. Two systems for substance encapsulation capable of external actuation were subsequently examined: amphiphilic nanoparticles embedded into vesicle membranes and amphiphilic tubules. These schemes differed most notably in that the hydrophilic and hydrophobic ligands on the surface of nanoparticles may dynamically redistribute in response to their surroundings<sup>7</sup> whereas the

ligands present on the interior and exterior of the tubules cannot, hence probing the differences between adaptive and static surface chemistries.

Previous research has demonstrated that amphiphilic nanoparticles fused with membrane bilayers of vesicles only if the particle were similar in size to the hydrophobic membrane core<sup>8</sup>, the membrane is denatured to ease penetration into vesicle walls<sup>9</sup>, or detergents were used to stabilize interactions<sup>10</sup>. The experiments detailed in this thesis were performed given the hypothesis that the hydrophilic and hydrophobic ligands on the surface of nanoparticles can rearrange in response to changes in environmental stimuli, allowing the hydrophobic ligands to interact favorably with the hydrophobic membrane core (Figure 1.1). Since the nanoparticles can tether to the vesicle via the hydrophobic groups, this would eliminate the size restriction and need for membrane disrupting additives.

While cylindrical particles have been shown to connect end-on-end at a liquid-air interface<sup>11</sup> and magnetic nanotubes with dual functionalization were loaded via preferential absorption of molecules treated with corresponding ligands<sup>12</sup>, limited research has focused on their potential self-assembly when submerged in mixtures of organic and aqueous phases. Several tests of varying tubule sizes examined the hypothesis that, in an effort to reduce their interfacial surface tension, the exposed solvents contained within functionalized tubules should form capillary “bridges” leading to end-on-end connections through which particles may flow (Figure 1.2). The movement of substances through the chain from one location to another would then be governed by internal capillary interactions rather than external forces.



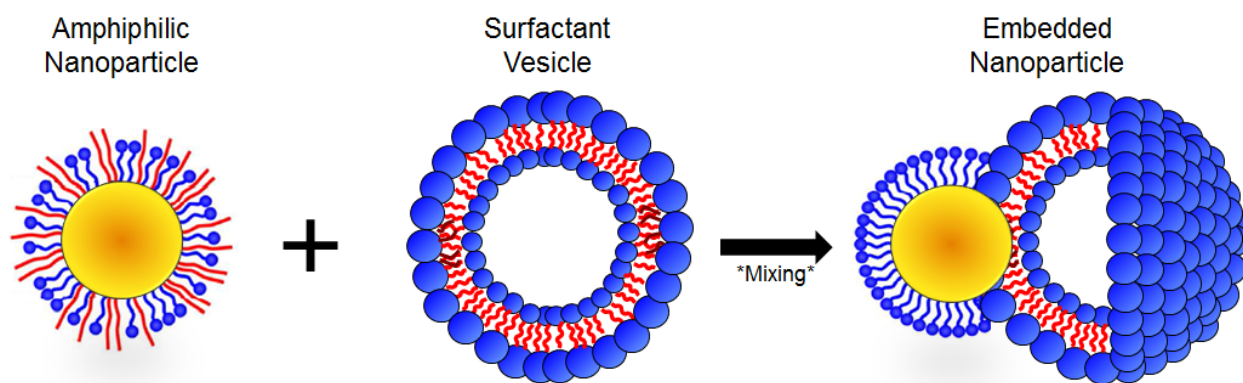


**Figure 1.1: Amphiphilic nanoparticle incorporation into surfactant vesicle schematic.**

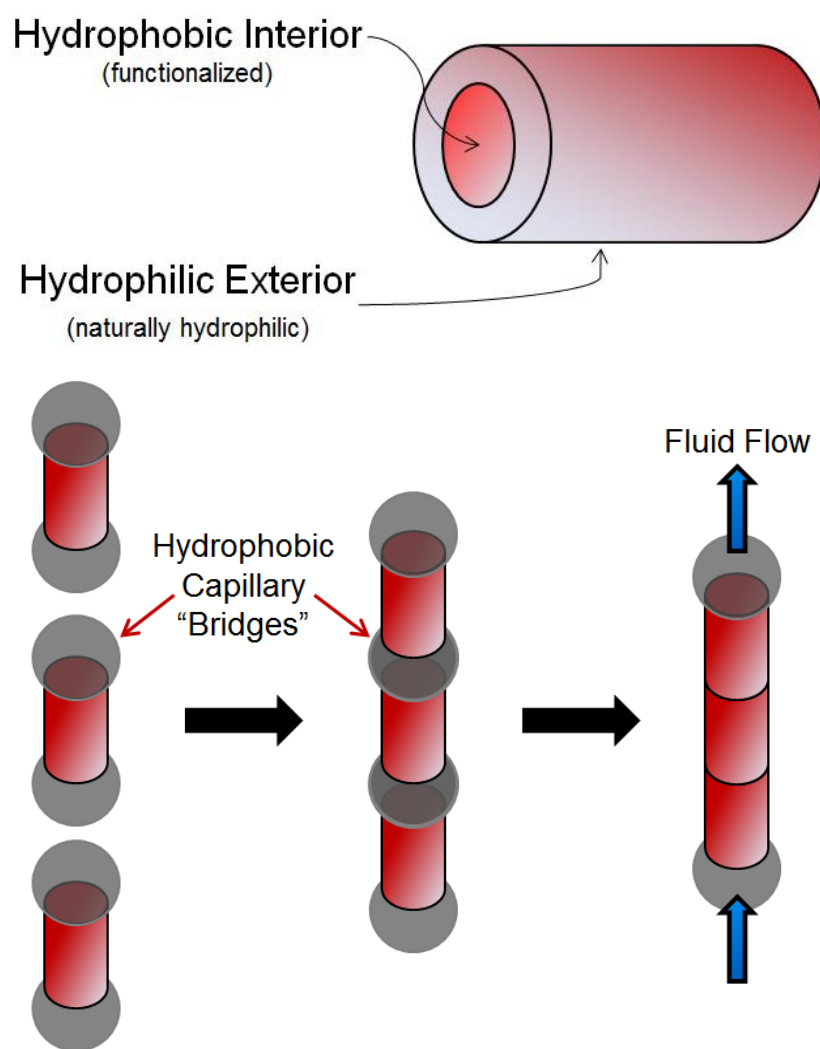


**Figure 1.2: Amphiphilic tubule arrangement into chains schematic.**

## Research Objectives

- 1<sup>st</sup> Goal: Demonstrate that amphiphilic nanoparticles larger than the membrane bilayer can be incorporated into surfactant vesicles without the need for denaturing agents
  - Hypothesis: Because the hydrophilic and hydrophobic ligands on the surface of nanoparticles can redistribute in response to changes in their environment, the hydrophobic ligands should interact with the hydrophobic membrane core and tether nanoparticles to vesicle walls – **Successful** (see results in Chapter 4)
- 2<sup>nd</sup> Goal: Show that amphiphilic tubules will arrange into end-on-end chains through which fluid can flow when submerged in a mixture of aqueous and organic phases
  - Hypothesis: The solvent contained within the tubes but exposed at the open ends should interact favorably with like solvents of other tubes to reduce their overall interfacial surface tension – **Unsuccessful** (but promising at the macro-scale, see Chapter 4)
- Thesis Organization:
  - Chapter 2 gives an overview of previous literature regarding amphiphilic nanoparticles and tubules
  - Chapter 3 details the experimental procedures performed to incorporate amphiphilic gold nanoparticles into surfactant vesicles and examine the assembly of amphiphilic tubules into chains
  - Chapter 4 presents and discusses the data obtained from the experiments
  - Chapter 5 reiterates the main results and offers brief extensions for future research

## CHAPTER 2

### **Relevant Literature on Amphiphilic Structures and their Self-Assembly**

This chapter gives an overview of recent literature exploring the rearrangement of ligands on amphiphilic nanoparticle surfaces and their incorporation into the membrane bilayers of vesicles. This is followed by an overview of recent literature analyzing the substance loading of functionalized tubules and the assembly of cylindrical particles at an interface of aqueous and organic phases.

#### Previous Nanoparticle Research

*Templated Synthesis of Amphiphilic Nanoparticles at the Liquid-Liquid Interface* (Andala et al. 2012)<sup>7</sup>

Amphiphilic nanoparticles composed of an inorganic metal core functionalized with hydrophilic mercaptoundecanoic acid (MUA) and hydrophobic 1,2-decanediol (DDT) were created with asymmetric surface chemistry as confirmed via contact angle measurements of nanoparticle monolayers. The amphiphilic nanoparticles spontaneously assembled at an interface of organic and aqueous liquids due to the ability of the ligands to rearrange on the surface of nanoparticles in response to environmental stimuli (the presence of the interface in this case). While a 1:1 ratio of ligands provided the optimum accumulation of nanoparticles at the interface, other ratios encouraged preferential dissolution into one phase of the mixture depending on the ligand in the majority. Future experiments and extensions involving different inorganic cores lead to natural applications in magnetic or optically responsive surfactants.

*Surface-structure-regulated cell-membrane penetration by monolayer-protected nanoparticles*

(Verma et al. 2008)<sup>10</sup>

Few nano-scale objects have been shown to avoid endosome formation and fully penetrate cell membrane without large disruptions or harsh chemical treatment. Cationic nanoparticles were synthesized and demonstrated to pass through cell membranes by creating transient holes depending on the size, shape, and composition of the nanomaterial in addition to its attached ligands. The membrane penetration of two nanoparticle isomers was examined, one with alternating anionic and hydrophobic functionalization and the other with random distribution of the same surface ligands. The nanoparticle with striations revealed the capacity to penetrate the membrane without bilayer disruption, which offers credence for further experiments and applications using nanoparticles of similar mixed surface chemistry.

*Multifunctional Lipid/Quantum Dot Hybrid Nanocontainers for Controlled Targeting of Live*

*Cells* (Gopalakrishnan et al. 2006)<sup>9</sup>

Hydrophobic quantum dots coated with phospholipids were incorporated into the bilayer membrane of lipid vesicles via membrane fusion upon mixing, as confirmed by confocal microscopy and fluorescence spectroscopy. These hybrid lipid/quantum dots did not exhibit typical cytotoxicity associated with quantum dots, making them fully biocompatible. The fluorescence of the quantum dots lends themselves toward easy observation and cellular imaging applications, while tests with different phospholipids confirm differing attachments are possible. As membranes can integrate any hydrophobic nanoparticles whose size matches or is smaller than the membrane thickness, this system offers great flexibility in manipulation for nano-scale

biotechnology, particularly given the premise of tunable association of the attached lipids to proteins and other molecules.

*Hydrophobic Gold Nanoparticle Self-Assembly with Phosphatidylcholine Lipid: Membrane-Loaded and Janus Vesicles* (Rasch et al. 2010)<sup>8</sup>

Hydrophobic gold nanoparticle with diameters of ~2 nm functionalized with DDT were successfully incorporated into phosphatidylcholine lipid vesicles via coextrusion (such that nanoparticles were contained beforehand within flat bilayers and remained encapsulated within the membrane walls upon vesicle formation) and detergent stabilization. The nanoparticles were also mixed with the lipid vesicles by dialysis, but the latter approach led to only partial loading of the vesicles with particles. Cryo-TEM analysis showed that the nanoparticles are embedded as a dense monolayer directly into the core of the lipid bilayer without apparent disruption of either the bilayer or lipid structure, but less than half of the vesicles actually contained any nanoparticles.

### Previous Tubule Research

*Magnetic Nanotubes for Magnetic-Field-Assisted Bioseparation, Biointeraction, and Drug Delivery* (Son et al. 2005)<sup>12</sup>

Silica ( $\text{SiO}_2$ ) nanotubes with an inner layer of magnetite ( $\text{Fe}_3\text{O}_4$ ) deposition were functionalized with hydrophobic octadecyltriethoxysilane (C-18 silane) and used for several molecule loading tests. A solution saturated with a hydrophobic dye was mixed with the synthesized nanotubes which were subsequently removed via application of an external magnetic field as confirmed by optical imagery and UV-Vis spectroscopy. Similarly, loading the nanotubes with human IgG, mixing with a solution of anti-human IgG, and separating the tubes with a magnetic field demonstrated loading of the tubes with the antibody as confirmed by fluorescence spectroscopy. As the tubes could also be loaded with ibuprofen coated with hydrophobic ligands and successively dissolved to release the contained molecules over time, this system's magnetic and adjustable functionalization can be easily extended to biocompatible drug delivery methods.

*Geometrically and Chemically Anisotropic Particles at an Oil-Water Interface* (Park et al. 2013)<sup>13</sup>

The arrangement of micron-sized amphiphilic cylinders at an interface of water and decane was analyzed via optical profilometry and electron microscopy upon encapsulation in a stable PDMS precursor gel. Varying the aspect ratio (ratio of the length to the diameter) revealed that while particles with small aspect ratios only arranged in upright configurations, high aspect ratios yielded tilted particles. These tilted particles could form assemblies with the titled cylindrical ends of other particles by reducing the interfacial deformation. Of note is that

although the particles were in contact, no direct end-on-end arrangements were observed (due to the resistance to unfavorable solvent association by the functionalized regions).

*Orientation and Self-Assembly of Cylindrical Particles by Anisotropic Capillary Interactions*

(Lewandowski et al. 2010)<sup>11</sup>

The spontaneous assembly of cylindrical microparticles into end-on-end chains or side-on-side lattices at a liquid-air interface was studied experimentally and computationally via examination of contact angles, aspect ratios, and interfacial distortions. Analysis revealed that the flat ends of the cylinders created excess area regions which acted as “bridges” to other cylinders. Connecting in end-on-end chains in the presence of fewer particles eliminated the interfacial tension of the system, while side-on-side connections in an abundance of particles were attributed to primarily capillary interactions. This chain assembly could be used to pass electric or other external signal along its length from one location to another.

## CHAPTER 3

### Experimental Procedures

This chapter presents the detailed experimental procedures for incorporating amphiphilic gold nanoparticles into surfactant vesicles and examining the end-to-end assembly of amphiphilic tubules of varying sizes.

#### Nanoparticles

*Gold Nanoparticle Seed Solution (AuDDA, ~2-4 nm)<sup>14</sup>:*

In a typical preparation, 23.6 mg of gold (III) chloride trihydrate ( $\text{HAuCl}_4 \cdot 3\text{H}_2\text{O}$ ), 222.1 mg of dodecylamine (DDA), and 277.1 mg of didodecyldimethyl ammonium bromide (DDAB) were added to a clean 20 mL vial along with ~5.78 g of toluene. After sonicating the vial for 10 minutes and the solution changed from light orange to pale yellow, the first solution was stirred at ~450 rpm using a ½” magnetic stir bar and stir plate. 58.6 mg of tetrabutylammonium borohydride (TBAB) and 110.9 mg of DDAB were then added to a second clean 20 mL vial along with ~2.49 g of toluene. After 10 minutes of sonication, the second solution was added to the first as quickly as possible using a disposable syringe. The initial vial was then sealed with Teflon tape and allowed to stir overnight (or for 12 hours).

*Gold Nanoparticle Growth Solution (AuDDA, ~6nm)<sup>15</sup>:*

223.1 mg of  $\text{HAuCl}_4 \cdot 3\text{H}_2\text{O}$ , 2.624 g of DDA, and 1.048g of DDAB were added to a clean Erlenmeyer flask along with ~49.61 g of toluene. The solution was stirred at ~450 rpm using a 1” magnetic stir bar and an upside down 20 mL vial as a cap. 1.048 g of DDAB was added along with ~19.16 g of toluene to another 20 mL vial and vortex mixed then sonicated for 2



minutes each. 145.0 mg of hydrazine ( $\text{N}_2\text{H}_4$ ) was then added to the vial and the solution was sonicated for another 10 minutes. The seed solution was fully added to the Erlenmeyer flask, and the hydrazine solution was then added dropwise using a glass pipette, slowly changing the purple color into a darker purple/red. The flask was capped with a 20 mL vial, sealed with Teflon tape, and allowed to stir overnight (or for 12 hours).

*Precipitation and Concentration Determination of AuDDA NPs<sup>14,15</sup>:*

After the growth and seed solutions were thoroughly reacted, excess methanol was added to the Erlenmeyer flask while stirring (as much as possible). The flask was then placed on a hood counter at room temperature overnight to allow the nanoparticles to settle to the bottom. The now clear top portion of the flask was removed and discarded using a glass pipette. After drying the remaining solution with a nitrogen stream, the nanoparticles were dispersed in toluene. The concentration was determined using UV-Vis and the Beer-Lambert law (with an extinction coefficient for AuNPs of  $3.050 \text{ M}^{-1}\text{cm}^{-1}$ ) after diluting the sample 200 times.

*Functionalization of AuMUA/ODT NPs<sup>16</sup>:*

In a typical preparation, 35.6  $\mu\text{mol}$  of octadecanethiol (ODT) dissolved in toluene (1.78 mL of a 20 mM solution) was added to 10  $\mu\text{mol}$  of AuDDA (0.5 mL of a 20 mM solution on a gold atom basis) in a clean 20 mL vial stirred for five minutes using a 1/2" magnetic stir bar. 4.44  $\mu\text{mol}$  of mercaptoundecanoic acid (MUA) dissolved in dichloromethane (0.222 mL of 20 mM solution) was then added to the solution. Stirring for 12 hours at 40 °C caused the particles to precipitate completely from solution. After decanting the supernatant, the now functionalized AuMUA/ODT particles were washed with toluene, dichloromethane, and then acetone to remove excess

ligands. After drying any remaining solution with a nitrogen stream, the nanoparticles were dissolved in 2 ml of deionized water. The pH was adjusted to  $>11$  by addition of tetramethylammonium hydroxide (TMAOH) to deprotonate the MUA ligands.

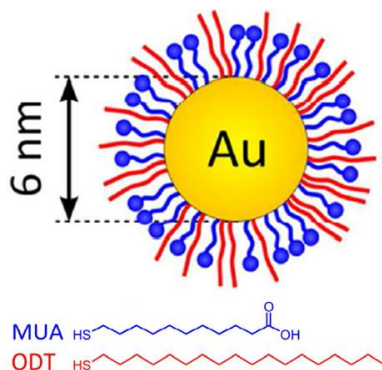


**Figure 3.1: AuMUA/ODT NP schematic.**

*Surfactant Vesicle Synthesis and NP Mixing*<sup>17,18</sup>:

A cationic surfactant (CTAT) and anionic surfactant (SDBS) were added in a CTAT/SDBS ratio of 30:70 (by weight) up to 1 wt% in deionized water with vigorous vortex mixing until homogenous solution with a bluish hue was created. Vesicles varied in diameter from  $\sim 50$ -150 nm. 1 mL of this vesicle solution was added to 1 mL of 1 mM AuMUA/ODT solution by vortex mixing for 5 minutes with the pH adjusted to  $>11$  by addition of TMAOH. tetramethylammonium chloride (TMACl) was added to reach an ionic strength of 100 mM by vortex mixing for 10 minutes to lessen electrostatic repulsions.

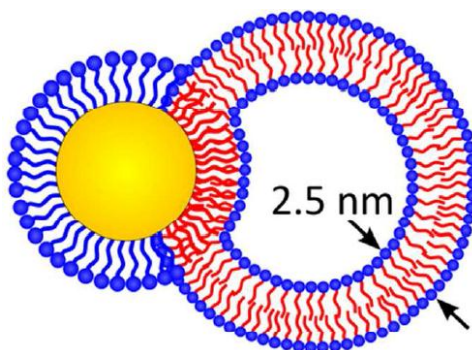


**Figure 3.2: AuMUA/ODT NP association with surfactant vesicle schematic.**

## Tubules

### *Micron-Sized Au/Fe<sub>2</sub>O<sub>3</sub> Tubes from Electrospun Fiber Templates<sup>19,20</sup>:*

360 mg of poly bisphenol A carbonate (PC) was dissolved in 2 mL of dichloromethane/dimethylformamide (DCM/DMF, 1.30/0.70). The polymer solution was electrospun using an applied voltage of 20 kV and distance between the spinneret and collector (aluminum foil) of 20 cm. Scissor-cut pieces of the foil and fibers were soaked for 1 minute in 1 M Hydrochloric Acid (HCl) and pulled from the collector foil. Separated fibers were sensitized in 3.0 mM tin (II) chloride dihydrate (SnCl<sub>2</sub>•2H<sub>2</sub>O) in 0.01 M HCl for 30 minutes and subsequently activated in 3.0 mM palladium (II) chloride (PdCl<sub>2</sub>) in 0.01 M HCl for another 30 minutes. After rinsing with deionized water, the fibers were soaked in 20 mL of 0.03 M HAuCl<sub>4</sub>•3H<sub>2</sub>O in H<sub>2</sub>O for 30 minutes to initiate electroless plating. The fibers were then placed in a buffered solution with pH 6.4, maintained using 0.4 M citric acid and 1 M potassium hydroxide (KOH), to which 20 mL of 0.1 M sodium L-ascorbate was added for 30 minutes. To add another iron oxide layer to the gold-coated fibers, the fibers were simply dipped into a solution containing 0.8 g of iron (III)-acetylacetonate dissolved in isopropanol after filtration with a 0.22-μm Millipore filter. The polymer fiber templates were removed by pyrolysis at 650 °C for 1 hour (with steady heating and cooling).

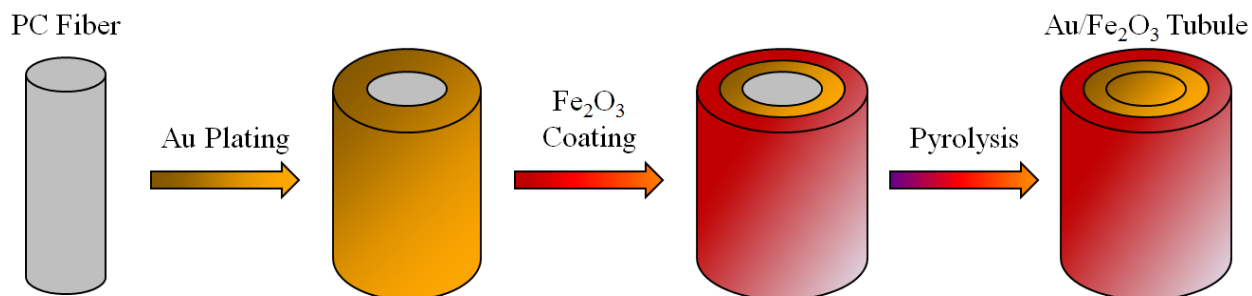


**Figure 3.3: Au/Fe<sub>2</sub>O<sub>3</sub> Tubules from electrospun polycarbonate fiber schematic.**

Functionalization was attempted by addition of the tubes to solutions of cinnamic acid and 1,2-decanediol (DDT) in excess by a factor of 10 in 5 mL of deionized water and toluene, respectively, to make the interior hydrophilic and the exterior hydrophobic.

*SiO<sub>2</sub>/Fe<sub>3</sub>O<sub>4</sub> Nanotubes from Alumina Membrane Templates<sup>12,21,22</sup>:*

A 25 mm Whatman Anodisc membrane (pore size ~175 nm) was immersed in a silicon tetrachloride (SiCl<sub>4</sub>) in 67.0 mol% carbon tetrachloride (CCl<sub>4</sub>) solution for 2 minutes and washed with CCl<sub>4</sub> to remove excess reagent. The membrane was then placed in a petri dish containing fresh CCl<sub>4</sub> for 15 minutes to remove unbound SiCl<sub>4</sub>. Remaining CCl<sub>4</sub> was displaced by soaking in a 1:1 CCl<sub>4</sub>/methanol solution for 2 minutes, followed by soaking in ethanol for 5 minutes. The membrane was fully dried using a nitrogen stream, then immersed in deionized water for 5 minutes, followed by methanol for 2 minutes. The membrane was then dried using a nitrogen stream again, and the entire process was repeated 20 times to achieve optimal silica growth (~20-25 nm tube diameter). Magnetite was added to the interior of the tubes by soaking the membrane in 4.0 mL of 1.0 M FeCl<sub>3</sub> (in 250 mL of 2 M HCl) and 1.0 mL of 2.0 M FeCl<sub>2</sub> (in 100 mL of 2 M HCl) for 2 minutes, followed by soaking in 1 M ammonium hydroxide (NH<sub>4</sub>OH) for 5 minutes. Excess deposition was removed by thorough washing with deionized water and manual scraping via a wet cotton swab. Additional polishing was performed using a cotton swab and ~35 µm silica carbide pellets in 3 mL of deionized water for 20 minutes. The tubes were removed by dissolving the alumina template in 50% hydrosulfuric acid for 2 days and collected by centrifugation. Functionalization was attempted by the addition of DDT in excess by a factor of 5 in toluene to make the interior hydrophobic while the exterior would remain naturally hydrophilic.

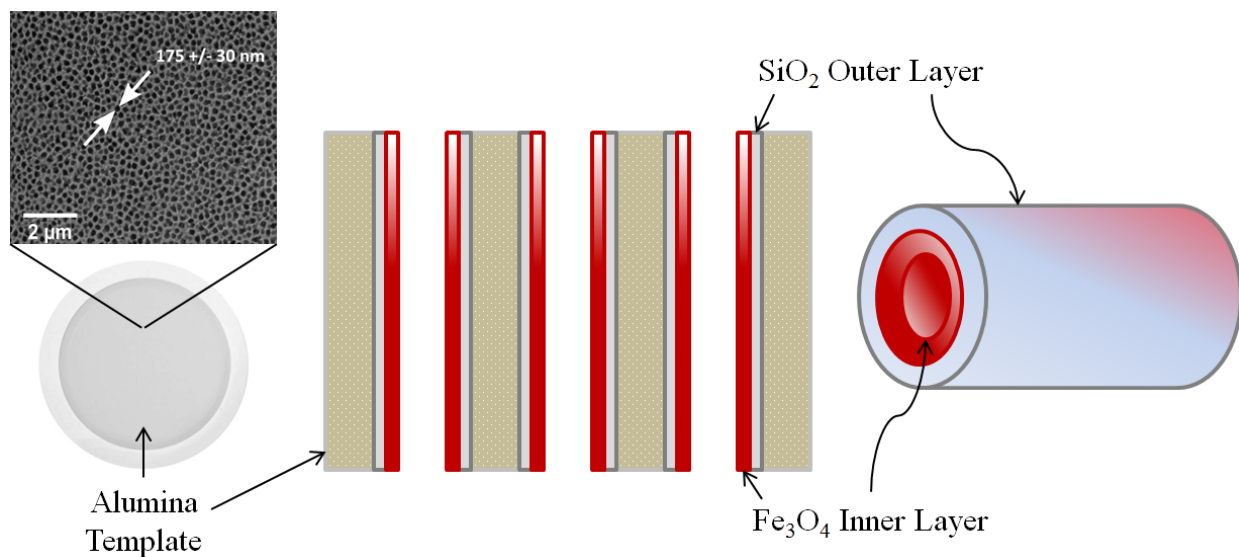


**Figure 3.4:  $\text{SiO}_2/\text{Fe}_3\text{O}_4$  nanotubes from alumina template schematic.**

*Millimeter-Sized Borosilicate Glass Capillary Tubes with Hydrophobic Interiors*<sup>12,13,23</sup>:

Glass capillary tubes with outer diameter of  $\sim 0.65$  mm and inner diameter  $\sim 0.45$  mm were functionalized internally using 100 mM octadecyltriethoxysilane (C18-Silane) in toluene by allowing the tubes to draw up the solution via capillary action and soaking in place for 2 hours. After drawing out the toluene by contact with a disposable Kimwipe, the tubes were then cut into  $\sim 0.5$  cm pieces using a Shortix Capillary Column Cutter to score the glass before manually breaking the glass by hand (edges were examined under the microscope attachment of the cutter to ensure even breakage). The tubes were placed in a petri dish filled with water after being refilled with toluene (which easily coated the entire interior and indicated proper functionalization) and moved as groups by end-to-end hydrophobic interactions. Future experiments will involve bubbling in carbon dioxide to and from two feed lines to a salt water solution (for higher buoyancy) to test whether air filled tubes will spontaneous arrange into channels from one hydrophobic fluid source to another.

## CHAPTER 4

### Results and Discussion

This chapter discusses the results of the experiment to incorporate amphiphilic nanoparticles into surfactant vesicles and assemble amphiphilic tubules into end-on-end chains comprising a larger fluidic channel. Briefly, amphiphilic nanoparticles approximately twice the size of the membrane bilayers of were successfully embedded into the walls of surfactant vesicles, while only preliminary macro-scale tubule tests showed evidence of end-to-end association.

#### Nanoparticles<sup>24</sup>

As suggested by Transmission Electron Microscopy (TEM) and confirmed via Cryo-TEM imagery, AuMUA/ODT nanoparticles interact with the hydrophobic core of surfactant vesicles under basic conditions with added salt (Figure 4.1).

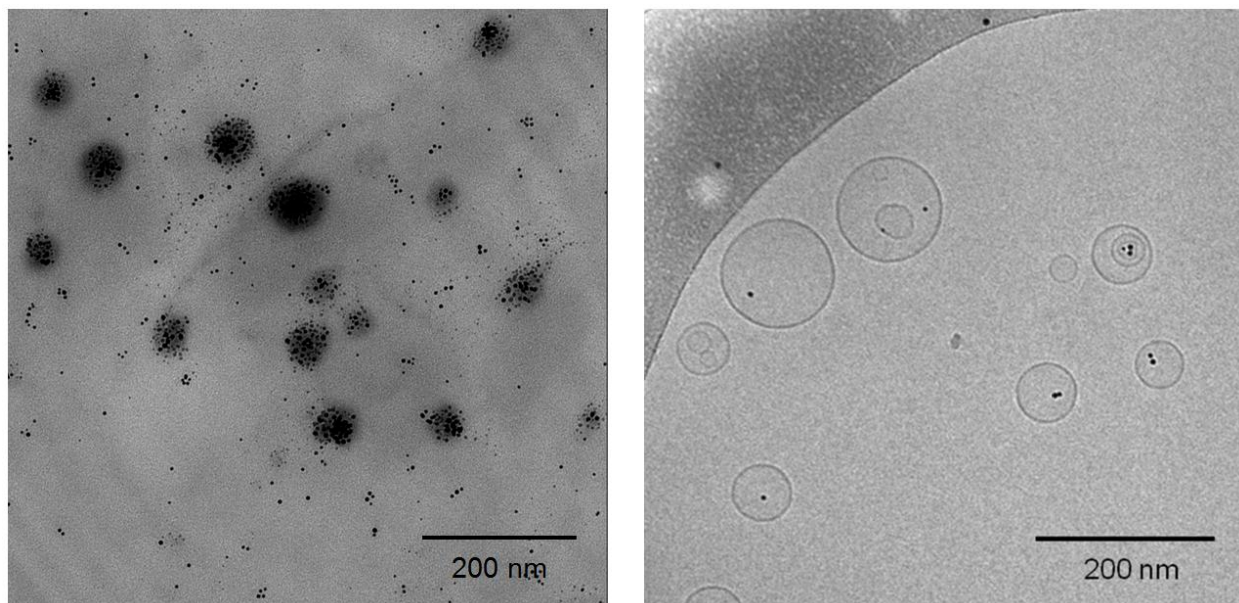


**Figure 4.1: TEM (left) and Cryo-TEM (right) images of AuMUA/ODT NPs and surfactant vesicles with 100 mM added TMACl. In TEM, the darker spots with NP aggregations represent surfactant vesicles.**

Important to note is that in dry TEM, the vesicles appear to contain many nanoparticles presumably due to a drying effect whereby nanoparticles move to areas where liquid remains as it evaporates (as in the vesicles themselves). While TEM can show preferential association, Cryo-TEM of a cross-section of the vesicles and nanoparticles is required to confirm the interactions. The ratio of ODT to MUA ligands was chosen to be as high as possible (until precipitation from solution made the nanoparticles no longer soluble in water) in order to maximize ODT interactions with the hydrophobic membrane core. Electrostatic titrations of the nanoparticle ligands to determine the point of charge neutrality (measured by UV-Vis spectroscopy) revealed that optimally 35% of the nanoparticle surfaces were covered by ODT.

Due to the reversible binding of the ligands to the nanoparticles, AuMUA/ODT nanoparticles arrange into small clusters in order to shield their hydrophobic ODT ligands from the surrounding water, as demonstrated by TEM and dynamic light scattering (DLS) data (Figure 4.2).

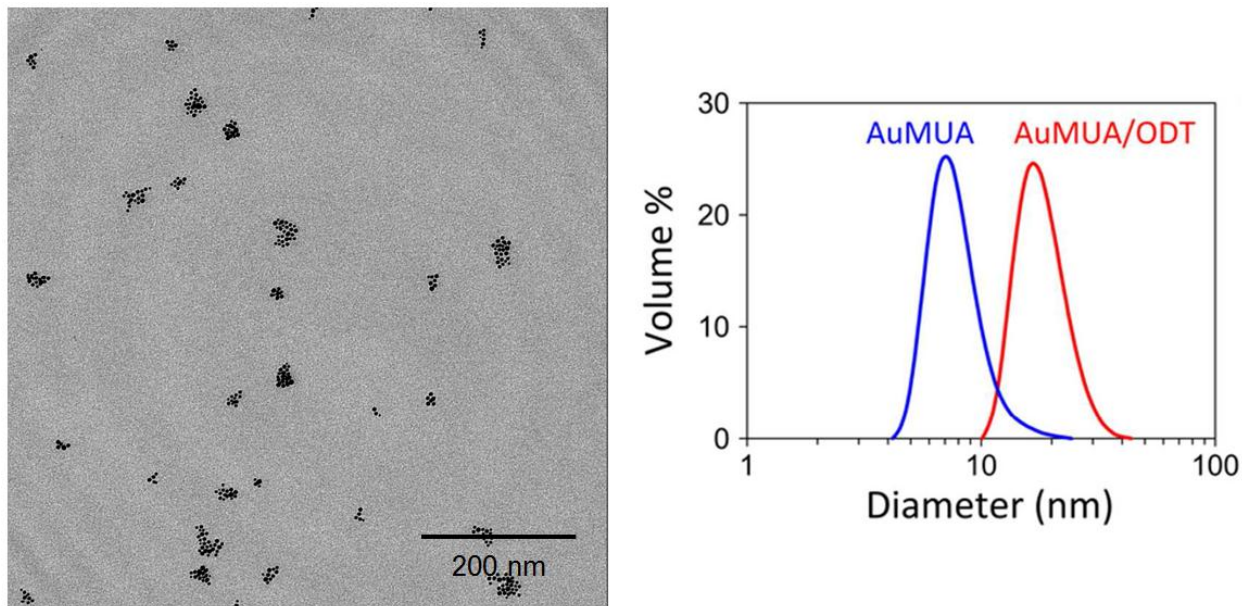


**Figure 4.2: TEM imagery (left) for AuMUA NPs in pH 11 water and DLS data (right) for AuMUA and AuMUA/ODT NPs in pH 11 water. The increased cluster size of ~18 nm for AuMUA/ODT is expected due to shielding of the hydrophobic ligands.**

AuMUA nanoparticles, on the other hand, revealed no cluster formation or association with vesicles as shown by TEM and Cryo-TEM images (Figure 4.3). AuODT nanoparticles, even when mixed with vesicles, simply precipitated from solution.



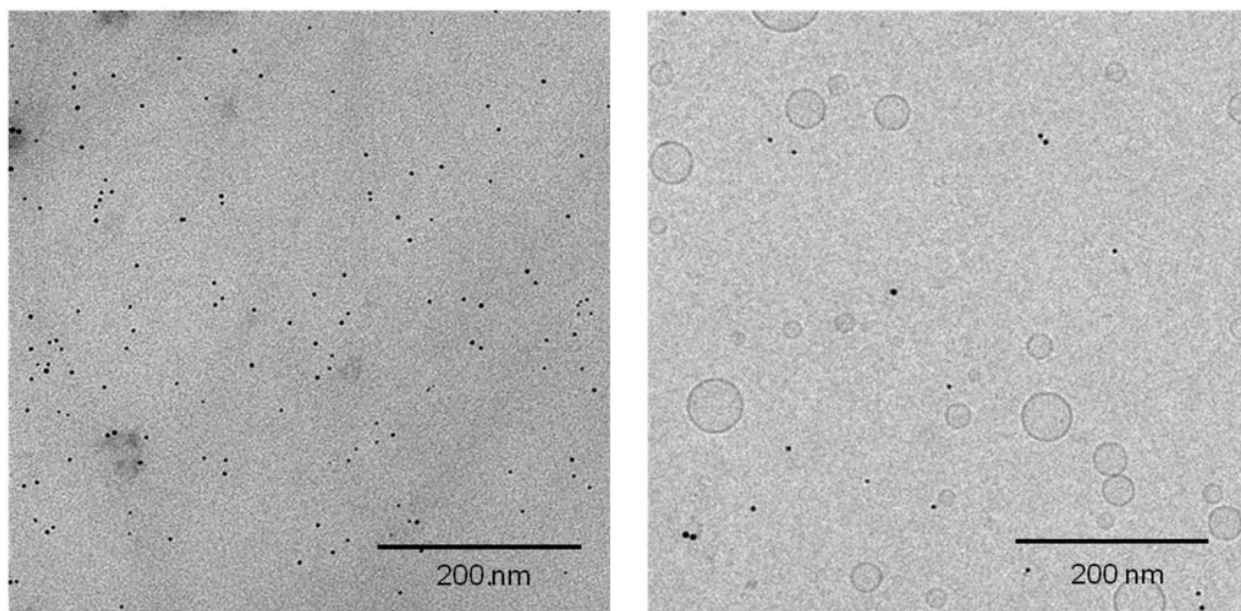


**Figure 4.3: TEM imagery (left) of AuMUA NPs and Cryo-TEM imagery (right) of AuMUA NPs with surfactant vesicles.**

In the absence of salt, nanoparticles no longer associated with the surfactant vesicles. This observation is confirmed both by Cryo-TEM imagery and zeta-potential measurements which show separate peaks without salt added and only one peak with salt addition (Figure 4.4).

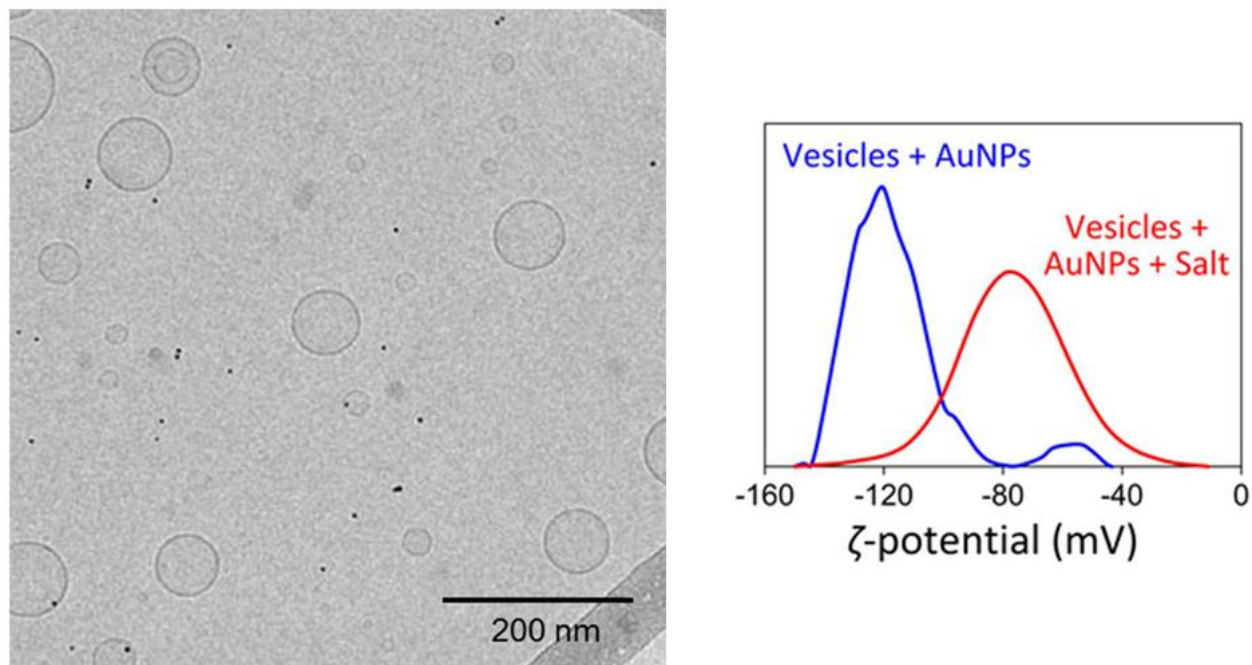


**Figure 4.4: Cryo-TEM imagery (left) of AuMUA/ODT NPs without added salt. Zeta-potential data (right) shows separate peaks near -120 mV and -60 mV for AuMUA/ODT NPs mixed with surfactant vesicles without added salt, while only one peak near -80 mV is observed when salt is added.**

The salt acts to decrease the electrostatic repulsions between the nanoparticle ligands and the vesicles such that the screening decreases to  $\sim 1$  nm (comparable to the ligand length). Since the nanoparticles and vesicles remain negatively charged even after the addition of salt, the favorable association can be attributed solely to hydrophobic interactions.

## Tubules

Dual metal tubules from electrospun fiber were created first due to their relative ease of synthesis and the possibility for different metal layers. The Au/Fe<sub>2</sub>O<sub>3</sub> tubules were analyzed by Scanning Electron Microscopy (SEM) and demonstrated high levels of melting and amalgamation between the metals as the dual layers appeared to be destroyed by pyrolysis (Figure 4.5).

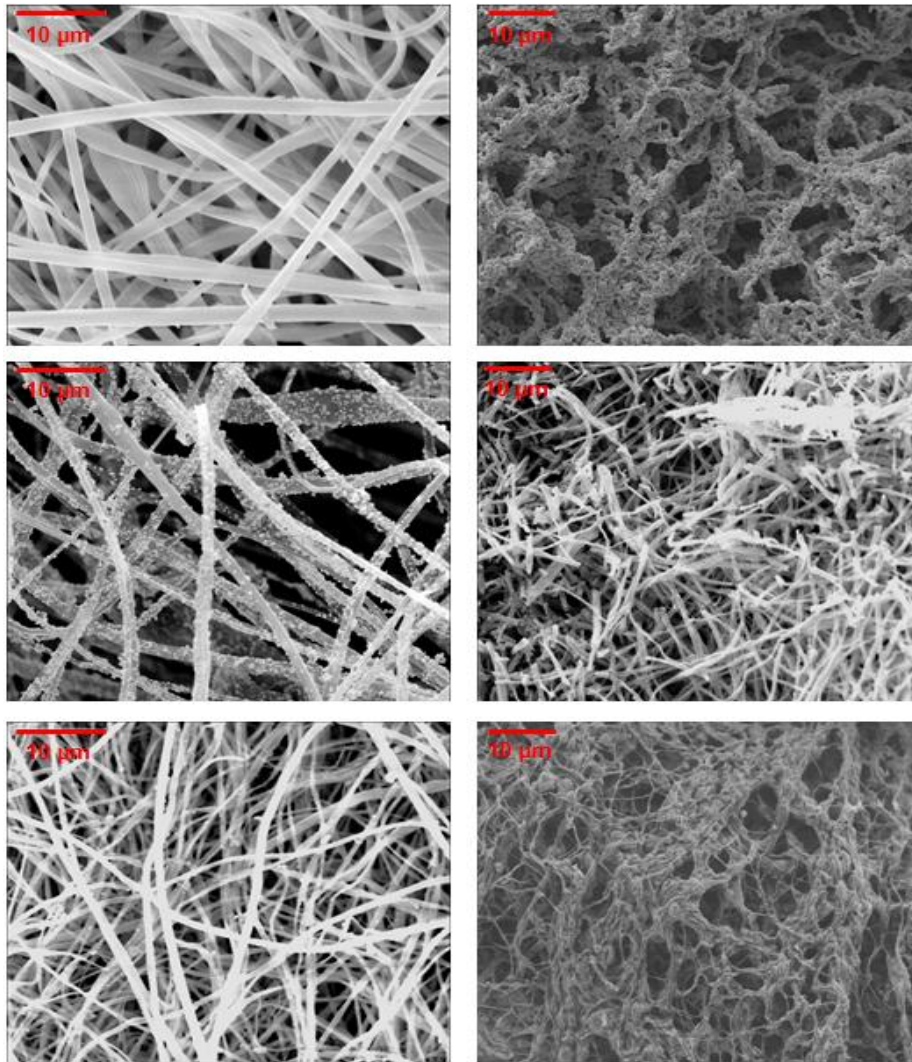


**Figure 4.5: SEM images of Au coated PC fibers (top left), Au tubules (top right), Fe<sub>2</sub>O<sub>3</sub> coated PC fibers (middle left), Fe<sub>2</sub>O<sub>3</sub> tubules (middle right), Au/Fe<sub>2</sub>O<sub>3</sub> coated PC fibers (bottom left), and Au/Fe<sub>2</sub>O<sub>3</sub> tubules (bottom right).**

The thermal degradation was confirmed by Energy Dispersive X-Ray Spectroscopy (EDS) which revealed no carbon signatures (Figure 4.6).  $\text{Fe}_2\text{O}_3$  tubules showed a hollow interior, while just Au tubules portrayed the same deformation as combined Au/ $\text{Fe}_2\text{O}_3$  tubules (Figure 4.5).

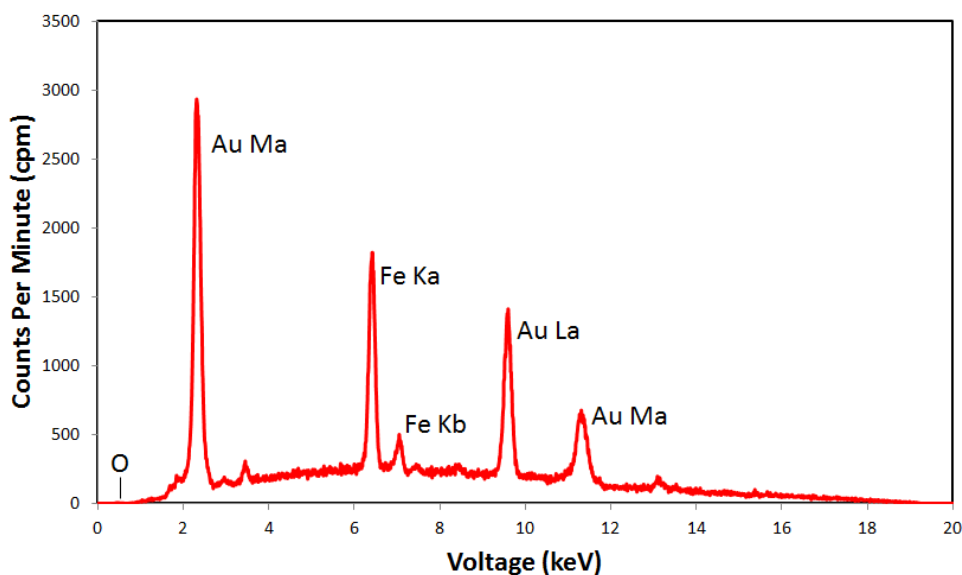


**Figure 4.6: EDS spectrum for Au/ $\text{Fe}_2\text{O}_3$  tubules.**

Although the  $\text{Fe}_2\text{O}_3$  and Au/ $\text{Fe}_2\text{O}_3$  tubes did organize at an interface of toluene and water, the successfully functionalized areas were most likely only the  $\text{Fe}_2\text{O}_3$  with attached hydrophobic DDT ligands. This presumption is based on only  $\text{Fe}_2\text{O}_3$  tubes being successfully created and because the tubes would disperse well in toluene but generally precipitate in water (with some smaller pieces floating by buoyant forces). Since the functionalization was unclear, the dual metal structure was largely eliminated, and the sonication to create smaller tubes broke the metals into uneven pieces, this experiment was replaced by one in which tubules had been consistently created in other literature.

Tubes from alumina templates were examined next due to their smaller size lending to easier biological incorporation and the tunable thickness depending on the number of deposition cycles. The  $\text{SiO}_2/\text{Fe}_3\text{O}_4$  nanotubes were analyzed by Optical Microscopy, SEM, and TEM to



determine in particular the efficacy of the magnetite deposition. Optical images revealed the issue that large chunks of tubes remained attached, either to portions of the alumina membrane not fully dissolved or to excess magnetite and silica deposition (Figure 4.7).

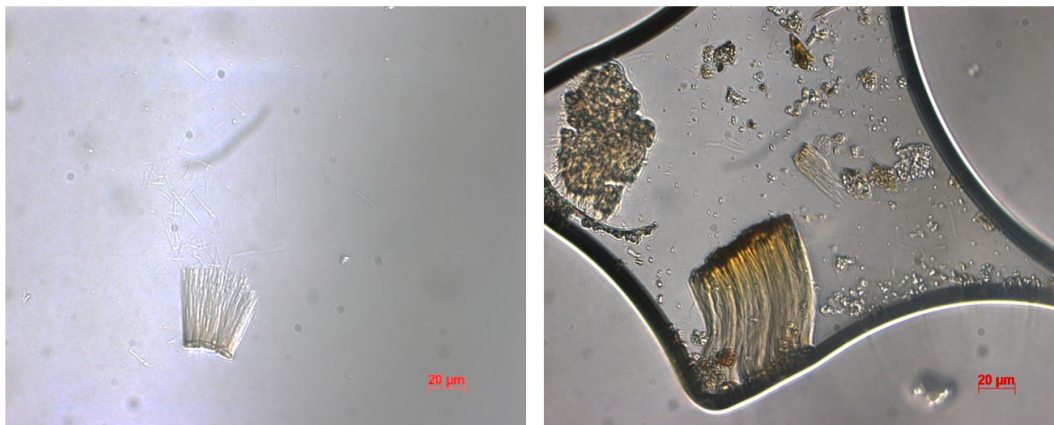


**Figure 4.7: Microscope images of  $\text{SiO}_2/\text{Fe}_3\text{O}_4$  nanotubes dispersed in water. Note the large conglomerations of tubes bundled more closely at one end assumed to be the top of the alumina membrane.**

Physical polishing with silica carbide particles eliminated enough of this deposition, as shown in SEM images of before and after the polishing, to obtain sufficient nanotube yields for subsequent analysis (Figure 4.8).

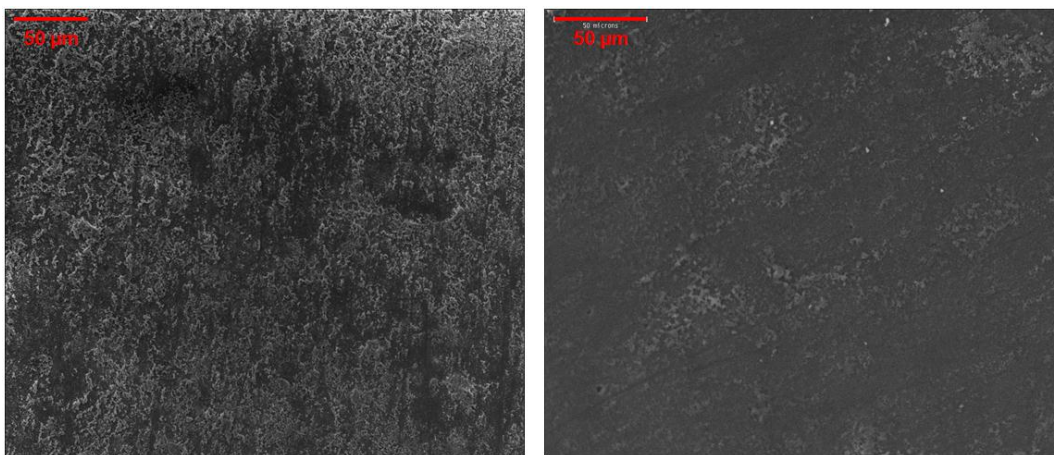


**Figure 4.8: SEM images of alumina template after  $\text{SiO}_2$  and  $\text{Fe}_3\text{O}_4$  deposition without polishing (left) and with polishing by SiC pellets for 20 minutes (right).**

TEM images demonstrated successful silica nanotube preparation, but magnetite deposition was unclear (Figure 4.9). The indistinct magnetite was mostly due to the fact that it deposits as ~20 nm particles, rather than one continuous metal film, which are not distinguishable via TEM.

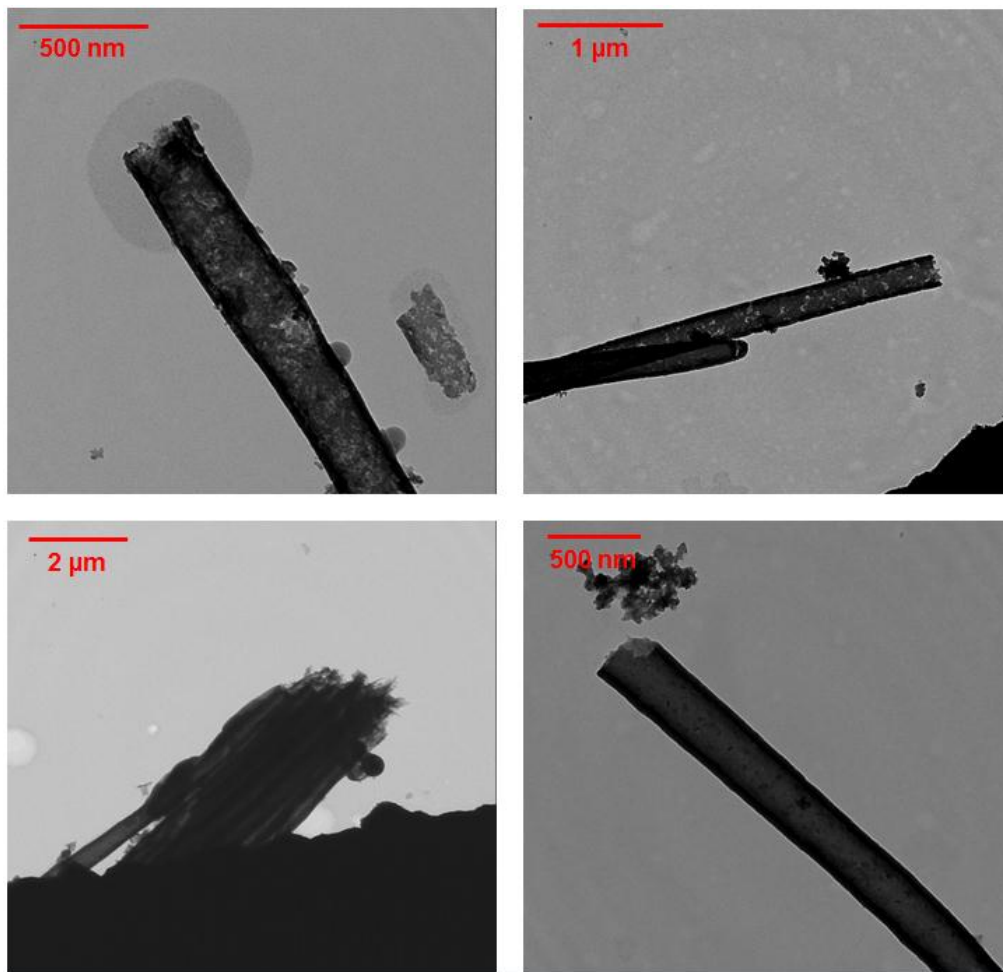


**Figure 4.9: TEM images of SiO<sub>2</sub> only nanotubes (left hand column) and SiO<sub>2</sub>/Fe<sub>3</sub>O<sub>4</sub> nanotubes (right hand column).**

As seen by microscope examination, this led to an apparent lack of toluene association with the nanotubes because there was either not enough DDT attaching on the interior of the tubes to capture toluene or due to the lack enough toluene near the open ends of the tubes to interact with nearby tubes and minimize their interfacial energy. Thus, this experiment was put on hold to explore a simplified macro-scale analysis of the system.

Due to the unsuccessful results with both micrometer and nanometer sized tubules, millimeter sized capillary tubes were analyzed in order to see quickly and clearly by eye whether the hypothesized interactions existed at all. When submerged in water on the bottom of a petri dish, functionalized capillary tubes filled with toluene did connect end-to-end when placed near each other. Moreover, the tubes even dragged each other along when manually moved by tweezers, demonstrating some favorable interaction between the open ends. To eliminate any Van der Waals interactions between the glass of the tubes and petri dish, the experiment will be repeated by filling the tubes with air (still hydrophobic relative to the water) and using a large beaker filled with salt water so that the increased buoyancy may suspend the tubes in solution. Upon adding syringes to pump carbon dioxide to and from solution across from each other and mixing the tube and salt water solution, the tubes will hopefully align with the tubes flowing carbon dioxide and allow for the flow of gas through the solution. Though the original tubule ideas made use of incorporated magnetic properties as a means to tailor particle flow, the presence of a gas or liquid feed should serve a similar function.

## CHAPTER 5

### Conclusion

Amphiphilic gold nanoparticles functionalized with hydrophilic MUA and hydrophobic ODT ligands were successfully incorporated into the walls of surfactant vesicles upon mixing with added salt. Dry TEM imagery suggested favorable association between AuMUA/ODT nanoparticles and vesicles which was confirmed in solution by Cryo-TEM imagery and DLS data. As the ligands can redistribute on the surface of nanoparticles in response to environmental stimuli, the ODT ligands could rearrange to interact with the hydrophobic membrane core and attach nanoparticles to the vesicles. This tethering via the ODT allowed for nanoparticles approximately twice the size of the membrane bilayer to be incorporated without denaturing agents. Future research involving magnetic nanoparticle cores would allow for direct control over the system, made all the better by the need for less powerful magnetic fields due to the larger particles.

Although nano-scale and micro-scale experiments yielded few positive results, investigation into the self-assembly of tubules with differing internal and external functionalization was much more promising at the macro-scale. Millimeter diameter glass tubes with hydrophobic interiors filled with toluene did drag along other tubes, presumably due to attraction by both favorable shielding of hydrophobic ends from water and an overall decrease in their interfacial surface tension. Further tests of these tubes using a more buoyant solution and carbon dioxide streams will hopefully demonstrate tubule chain formation dictated by fluid flow. Future experiments could then ideally downsize the system and incorporate magnetic properties via multiple tubule layers to allow for control of fluid movement through arrangement alteration via externally applied magnetic fields.



## REFERENCES

- <sup>1</sup>Wang, C.; Wang, Z.; Zhang, X. *Accounts of Chemical Research* **2011**, 45, 608.
- <sup>2</sup>Dirksen, A.; Langereis, S.; de Waal, B. F. M.; van Genderen, M. H. P.; Hackeng, T. M.; Meijer, E. W. *Chem. Comm.* **2005**, 22, 2811.
- <sup>3</sup>Ryadnov, M. G. *Angew. Chem., Int. Ed.* **2007**, 46, 969.
- <sup>4</sup>Stadler, B.; Bally, M.; Greishaber, D. Voros, J.; Brisson, A.; Grandin, H. M. *Biointerphases* **2006**, 1, 142.
- <sup>5</sup>Wu, G. H.; Milkhailovsky, A.; Khant, H. A.; Fu, C.; Chiu, W.; Zasadzinski, J. A. *J. Am. Chem. Soc.* **2008**, 130, 8175.
- <sup>6</sup>Kelly, K. L.; Coronado, E.; Zhao, L. L.; Schatz, G. C. *J. Phys. Chem. B.* **2003**, 107, 668.
- <sup>7</sup>Andala, D. M.; Shin, S. H. R.; Lee, H. Y.; Bishop, K. J. M. *ACS Nano* **2012**, 6, 1044.
- <sup>8</sup>Rasch, M. R.; Rossinyol, E.; Hueso, J. L.; Goodfellow, B. W.; Arbiol, J.; Korgel, B. A. *Nano Lett.* **2010**, 10, 3733.
- <sup>9</sup>Gopalakrishnan, G.; Danelon, C.; Izewska, P.; Prummer, M.; Bolinger, P. Y.; Geissbuhler, I.; Demurtas, D.; Dubochet, J.; Vogel, H. *Angew. Chem., Int. Ed.* **2006**, 45, 5478.
- <sup>10</sup>Verma, A.; Uzon, O.; Hu, Y. H.; Hu, Y.; Han, H. S.; Watson, N.; Chen, S. L.; Irvine, D. J.; Stellacci, F. *Nature Mater.* **2008**, 7, 588.
- <sup>11</sup>Lewandowski, E. P.; Cavallaro, M.; Botto, L.; Bernate, J. C.; Garbin, V.; Stebe, K. J. *Langmuir* **2010**, 26, 15142.
- <sup>12</sup>Son, S. J.; Reichel, J.; He, B.; Schuchman, M.; Lee, S. B. *J. Am. Chem. Soc.* **2005**, 127, 7316.
- <sup>13</sup>Park, B. J.; Choi, C. H.; Kang, S. M.; Tettey, K. E.; Lee, C. S.; Lee, D. *Soft Matter* **2013**, 9, 3383.
- <sup>14</sup>Jana, N. R.; Peng, X. G. *J. Am. Chem. Soc.* **2003**, 125, 14280.

- <sup>15</sup>Kalsin, A. M.; Fialkowski, M.; Paszewski, M.; Smoukov, S. K.; Bishop, K. J. M.; Grzybowski, B. A. *Science* **2006**, 312, 420.
- <sup>16</sup>Wang, D. W.; Nap, R. J.; Lagzi, I.; Kowalczyk, B.; Han, S. B.; Grzybowski, B. A.; Szleifer, I. *J. Am. Chem. Soc.* **2011**, 133, 2192.
- <sup>17</sup>Lee, J. H.; Gustin, J. P.; Chen, T. H.; Payne, G. F.; Raghavan, S. R. *Langmuir* **2005**, 21, 26.
- <sup>18</sup>Lee, J. H.; Agarwal, V.; Bose, A.; Payne, G. F.; Raghavan, S. R. *Phys. Rev. Lett.* **2006**, 96.
- <sup>19</sup>Ochanda, F.; Jones, W. E. *Langmuir* **2005**, 21, 10791.
- <sup>20</sup>Pal, B. ; Sharon, M. *Thin Solid Films* **2000**, 379, 83.
- <sup>21</sup>Kovtyukhova, N. I.; Mallouk, T. E.; Mayer, T. S. *Adv. Mater.* **2003**, 15, 780.
- <sup>22</sup>Berger, P.; Adelman, N. B.; Beckman, K. J.; Campbell, D. J.; Ellis, A. B.; Lisensky, G. C. *J. Chem. Ed.* **1999**, 76, 943.
- <sup>23</sup>Cubaud, T.; Ho, C. M. *Phys. Fluids* **2004**, 16, 4575.
- <sup>24</sup>Lee, H. Y.; Shin, S. H. R.; Abezgauz, L. L.; Lewis, S. A.; Chirsan, A. M.; Danino, D. D.; Bishop, K. J. M. *J. Am. Chem. Soc.* **2013**.

## ACADEMIC VITA

### Sean Austin Lewis

sal5290@psu.edu  
(610) 212-0953

#### Permanent Address:

1835 Arch Street, Suite 902  
Philadelphia, PA 19103  
(610) 212-7727

#### Campus Address:

302 Brill Hall  
University Park, PA 16802  
(610) 212-0953

---

### EDUCATION

**The Pennsylvania State University, Schreyer Honors College**  
B.S. Chemical Engineering with Honors  
Research Intensive Option

University Park, PA  
Expected May 2013

*Graduate Coursework:* General Transport Phenomena, Surface Characterization of Materials

*Publications:* Lee, H. Y.; Shin, S. H. R.; Abezgauz, L. L.; Lewis, S. A.; Chirsan, A. M.; Danino, D. D.; Bishop, K. J. M. "Integration of gold nanoparticles into bilayer structures via adaptive surface chemistry". *J. Am. Chem. Soc.* Revision Submitted: 25 March 2013.

### SKILLS

**Software:** SolidWorks, MatLab, Mathematica

**Technical:** Scanning Electron Microscopy, Transmission Electron Microscopy, Ultraviolet-Visible Spectroscopy, Goniometer, Zeta-Sizer

### EXPERIENCE

**The Pennsylvania State University**  
University Park, PA

May 2011 – August 2011, May 2012 – August 2012  
40 Hours Per Week

*Undergraduate Researcher (also during semesters for credit)*

- Explored the spontaneous self-assembly of amphiphilic nanoparticles into micellar and chain structures
- Examined the effects of ligand type, size, and ratio on embedding nanoparticles into vesicle membranes for applications in imaging and controlled substance release
- Investigated the self-assembly of functionalized magnetic nanotubes into nano-fluidic channels for controlled particle transport

### ORGANIZATIONS

- National American Institute of Chemical Engineers, September 2009 - Present
- National Society of Collegiate Scholars, April 2010 - Present
- Sigma Alpha Pi Society of Leadership and Success, August 2010 - Present
- Omega Chi Epsilon Chemical Engineering Honors Society, March 2012 - Present
- Phi Sigma Pi National Honors Fraternity, February 2010 - Present
  - Class Secretary, Spring 2010
  - Rush/Public Relations Chair, Spring 2011
  - Risk Management Chair, Fall 2011

### AWARDS

- Bausch & Lomb Honorary Science Award, University of Rochester, June 2009
- Paul Morrow Engineering Scholarship, The Pennsylvania State University, August 2009 - Present
- Schreyer Honors College Scholarship, The Pennsylvania State University, August 2009 - Present
- The Lee and Mary Eagleton Award for Excellence in Engineering Design, The Pennsylvania State University, August 2012